

**Breast Cancer <sup>18</sup>F-ISO-1 Uptake as a Marker of Proliferation Status**

**Author list:** Elizabeth S. McDonald, MD, PhD<sup>1\*</sup>, Robert K. Doot, PhD<sup>1\*</sup>, Anthony J. Young, BS<sup>1</sup>, Erin K. Schubert, BS<sup>1</sup>, Julia Tchou, MD, PhD<sup>2</sup>, Daniel A. Pryma, MD<sup>1</sup>, Michael D. Farwell, MD<sup>1</sup>, Anupma Nayak, MBBS, MD<sup>3</sup>, Amy Ziober<sup>3</sup>, Michael D. Feldman, MD, PhD<sup>3</sup>, Angela DeMichele, MD<sup>4</sup>, Amy S. Clark, MD<sup>4</sup>, Payal D. Shah, MD<sup>4</sup>, Hsiaoju Lee, PhD<sup>1</sup>, Sean D. Carlin, PhD<sup>1</sup>, Robert H. Mach, PhD<sup>1</sup>, David A. Mankoff, MD, PhD<sup>1</sup>

**Author affiliations:** <sup>1</sup>Department of Radiology, <sup>2</sup>Department of Surgery, <sup>3</sup>Department of Pathology and Laboratory Medicine, <sup>4</sup>Department of Medicine, Perelman School of Medicine, University of Pennsylvania

\*Contributed equally to this work.

†**Correspondence:**

Elizabeth McDonald, MD, PhD, FSBI  
Assistant Professor of Radiology  
University of Pennsylvania  
3400 Spruce Street, 1 Silverstein  
Philadelphia, PA 19104  
P: 215.614.0124  
Fax: 215.662.7436  
[Elizabeth.mcdonald@pennmedicine.upenn.edu](mailto:Elizabeth.mcdonald@pennmedicine.upenn.edu)  
<https://orcid.org/0000-0002-7209-4216>

**Financial support:** Dr. McDonald was supported by Susan G. Komen Foundation (CCR 16376362, SAC130060) and American Roentgen Ray Society Scholar award. Dr. Doot was supported by NIDA (K01DA040023). The work was sponsored by National Center for Research Resources and the National Center for Advancing Translational Sciences, National Institutes of Health (UL1TR000003), U.S. Department of Energy (DE-SE0012476), Penn Radiology Department and NCI (P30 CA016520).

**Shortened Title:** Breast Cancer <sup>18</sup>F-ISO-1 Uptake vs. Ki-67

## ABSTRACT

The sigma-2 receptor is a potential *in vivo* target for measuring proliferative status in cancer. Dehdashti et al. established the feasibility of using *N*-(4-(6,7-dimethoxy-3,4-dihydroisoquinolin-2(1*H*)-yl)butyl)-2-(2-<sup>18</sup>F-fluoroethoxy)-5-methylbenzamide (<sup>18</sup>F-ISO-1) to image solid tumors in lymphoma, breast cancer, and head and neck cancer (1). Here we report results of the first dedicated clinical trial of <sup>18</sup>F-ISO-1 in women with primary breast cancer. Our study objective was to determine whether <sup>18</sup>F-ISO-1 PET could provide an *in vivo* measure of tumor proliferative status, and we hypothesized uptake would correlate with a tissue based assay of proliferation, namely Ki-67 expression.

**Methods** Twenty-eight women with 29 primary invasive breast cancers were prospectively enrolled in a clinical trial (NCT 02284919) between 3/2015 and 1/2017. Each received an injection of 278-527 MBq <sup>18</sup>F-ISO-1 followed by a 50-55 minute post-injection positron emission tomography-computed tomography (PET/CT) image of the breasts. *In vivo* uptake of <sup>18</sup>F-ISO-1 was quantitated by maximum standardized uptake values (SUV<sub>max</sub>) and distribution volume ratios (DVR) and was compared to *ex vivo* immunohistochemistry for Ki-67. Wilcoxon rank-sum test assessed uptake differences across Ki-67 thresholds and Spearman's correlation tested associations between uptake and Ki-67.

**Results** Tumor SUV<sub>max</sub> (median 2.0 g/mL, range 1.3-3.3 g/mL), partial volume corrected (PVC) SUV<sub>max</sub>, and SUV ratios were tested against Ki-67. Tumors stratified into the high Ki-67 ( $\geq 20\%$ ) group had SUV<sub>max</sub> greater than the low Ki-67 ( $< 20\%$ ) group (P=0.02). SUV<sub>max</sub> exhibited a positive correlation with Ki-67 across all breast cancer subtypes ( $\rho=0.46$ , P=0.01,  $n=29$ ). PVC SUV<sub>max</sub> was positively correlated with Ki-67 for invasive ductal carcinoma ( $\rho=0.51$ , P=0.02,  $n=21$ ). Tumor-to-normal-tissue ratios and tumor DVR did not correlate with Ki-67 (P>0.05).

**Conclusion** <sup>18</sup>F-ISO-1 uptake in breast cancer modestly correlates with an *in vitro* assay of proliferation.

**Key words** Breast cancer; sigma-2; TMEM-97, Proliferation; <sup>18</sup>F-ISO-1

## INTRODUCTION

Tumor proliferative status is a key measure of breast cancer aggressiveness. The pathologic gold standard for measuring breast cancer proliferation is Ki-67, a nuclear protein expressed in proliferating cells, especially in G<sub>2</sub>, M, and the latter half of S-phase, but absent in quiescent cells in the G<sub>0</sub>-phase (2, 3). High expression of Ki-67 in breast cancer is a prognostic marker associated with increased recurrence and decreased survival (4-7). Ki-67 is also predictive for breast cancer response to chemotherapy and other systemic therapies (8-10). In addition, Ki-67 can be an early indicator of response for estrogen receptor (ER)-targeted therapy of ER positive cancers (11-13).

The sigma-2 receptor ( $\sigma$ 2R) is a biomarker of proliferative status in cancer, validated in mammary adenocarcinoma cells *in vitro* (14), and solid tumors (15). A  $\sigma$ 2R-selective radioligand, *N*-(4-(6,7-dimethoxy-3,4-dihydroisoquinolin-2(1*H*)-yl)butyl)-2-(2-<sup>18</sup>F-fluoroethoxy)-5-methylbenzamide (<sup>18</sup>F-ISO-1), was developed to image  $\sigma$ 2R expression (16). The ability of <sup>18</sup>F-ISO-1 to measure  $\sigma$ 2R binding as an indicator of cellular proliferation was validated in pre-clinical models and revealed a linear relationship between <sup>18</sup>F-ISO-1 uptake and proliferative status of breast tumor xenografts (17). The gene coding for  $\sigma$ 2R is transmembrane protein 97 (*TMEM-97*) (18). *TMEM-97* is overexpressed in a variety of cancers, and linked to poor prognosis (19, 20). In a cellular model of breast cancer, expression of *TMEM-97* parallels radioligand binding of <sup>18</sup>F-ISO-1, and <sup>18</sup>F-ISO-1 correlates with tumor proliferative status as assessed by Ki-67 and other markers (21). The active form of  $\sigma$ 2R is in a ternary complex with progesterone receptor membrane component 1 and the low-density lipoprotein receptor that together increases the rate of cellular internalization of low-density lipoproteins (22).

Dehdashti et al. (1) identified  $\sigma$ 2R targeting <sup>18</sup>F-ISO-1 as a biomarker of proliferation in a mixed tumor population. The purpose of this study was to evaluate <sup>18</sup>F-ISO-1 in a cohort of 28 breast cancer patients to further evaluate the feasibility of using this PET radiotracer as an *in vivo* breast cancer proliferation biomarker.

## MATERIALS AND METHODS

## **Patient Population**

Patients were recruited and consented for the study, “<sup>18</sup>F-ISO-1 PET/CT in Breast Cancer” (NCT02284919), between March 2015 and January 2017, with study protocol information at [clinicaltrials.gov](http://clinicaltrials.gov). Key inclusion criteria were a new diagnosis of breast cancer with a single diameter of at least 1 cm on conventional imaging and no prior treatment. Candidates were identified at time of biopsy and consented after pathologic confirmation of disease. The study and informed consent were approved by the University of Pennsylvania Institutional Review Board and Cancer Center Clinical Trials Scientific Review and Monitoring Committee. All imaged subjects were included in this analysis and were  $\geq 18$  years old, not pregnant, willing to undergo a PET/CT scan, and signed written informed consent.

## **<sup>18</sup>F-ISO-1 PET/CT Imaging**

<sup>18</sup>F-ISO-1 was produced by the University of Pennsylvania Cyclotron Facility under US Pharmacopeia-compliant procedures, as previously described (23) and administered under a Food and Drug Administration approved exploratory investigational new drug application (#124129). The mean and standard deviation of the administered mass of <sup>18</sup>F-ISO-1 was  $2.8 \pm 2.6$   $\mu\text{g}$  (range 0.12–9.9  $\mu\text{g}$ ). The mean administered activity was  $468.16 \pm 54.18$  MBq (range 278–527 MBq). One-hour dynamic imaging of breasts was followed by a whole body static scan. There were no adverse or clinically detectable pharmacologic effects in any of the 28 subjects. No significant changes in vital signs were observed. All studies were on an Ingenuity TF PET/CT (Philips Healthcare, Cleveland, OH, USA) using previously described image reconstruction (24). Tumors’ static maximum and peak (25) values ( $\text{SUV}_{\text{max}}$  and  $\text{SUV}_{\text{peak}}$ ) and background uptake were measured from a summed 50–55 minute image. This time point was chosen to maximize uptake while compensating for inconsistent time bin lengths of the final frame. Non-specific binding of <sup>18</sup>F-ISO-1 in background was estimated from the average radiotracer concentration in normal tissue, calculated from a 15-mm diameter sphere placed on the contralateral breast or from a 20-mm sphere placed on the left latissimus dorsi. A smaller normal breast region was used to facilitate matching normal contralateral breast placement to tumor location. SUVs were measured using Pmod v3.7 image analysis software (PMOD

Technologies Ltd., Zurich, Switzerland), blinded to reference standard (Ki-67) data. Tumors were measured in three dimensions using magnetic resonance imaging and CT for partial volume correction (PVC). PVC of tumor radiotracer uptake was calculated as previously described (26) using normal breast background uptake and recovery coefficient curves measured using phantom images of spheres acquired on this study's PET/CT scanner. Imaging measures are reported as maximum standardized uptake values ( $SUV_{max}$ ), tumor-to-normal-breast ratios ( $SUV/NBr$ ) and tumor-to-normal-muscle ratios ( $SUV/NM$ ).

### **Kinetic Analyses**

Distribution volume ratios (DVR) were calculated for tumor  $^{18}F$ -ISO-1 peak uptakes using Pmod v3.7 image analysis software via the Logan reference tissue model (27) using normal breast as the reference tissue and using a  $k_2'$  calculated for each patient using Ichise's multilinear reference tissue model, employing a blood pool reference region measured via a left ventricle one  $cm^3$  peak volume of interest (28).

### **Immunohistochemistry (IHC)**

The Ki-67 index (fraction of proliferating cells) was assessed using the diagnostic protocol validated for clinical Ki-67 measurements. IHC for Ki-67 was performed on fixed whole slide tumor sections on an automated platform (Leica Bond-III<sup>TM</sup> instrument, IL, USA) using a monoclonal mouse antibody (Anti-Human Ki-67 Antigen, Clone MIB-1, Dako # IR626). Briefly, 5-micron thick unstained sections cut from formalin-fixed paraffin embedded tissue blocks were obtained on charged slides. Sections were de-paraffinized and hydrated, followed by heat induced epitope retrieval, treatment with low pH buffer and treatment with primary antibody for 15 minutes. Slides were rinsed with wash buffer and analyzed using the Bond Polymer Refine Detection System as per the manufacturer's instructions. Nuclear staining for Ki-67 was scored using Aperio image analysis platform (Leica Biosystems Imaging, Vista, CA, USA). Appropriate positive (tonsil) and negative reagent controls were evaluated. Automated IHC image analysis counting > 1000 nuclei was utilized, following the guidelines of the *International Ki-67 in Breast Cancer Working Group* and reported as the percentage of nuclei positive for Ki-67 (4).

## Statistical Analyses

We hypothesized that  $^{18}\text{F}$ -ISO-1 PET uptake measures quantitative *in vivo* breast cancer proliferative status and tested for correlations between Ki-67 score as a biomarker for proliferation and  $^{18}\text{F}$ -ISO-1 uptake. Statistical analyses were performed using IBM SPSS 25 (Armonk, NY, USA). Spearman's rank correlation was used to estimate the strength of association between tracer uptake and Ki-67. The threshold for "high" versus "low" Ki-67 was defined as 20%, based on a 2017 study of early stage breast cancers (29) and the 2015 St. Gallen meeting consensus (30). In addition a 14% Ki-67 threshold was also examined based on the earlier 2011 St. Gallen meeting consensus (31). Wilcoxon rank-sum tests were used to compare tracer uptake between "high" ( $\text{Ki-67} \geq 14\%$  or  $20\%$ ) and "low" ( $\text{Ki-67} < 14\%$  or  $20\%$ ) proliferation tumors. Analyses were repeated in invasive ductal and ER positive tumors. Statistical significance was assessed based on a two-sided alpha of 0.05. The sample size was estimated to provide 80% power to detect a correlation of 0.47 using a 5% type I error rate (two-tailed).

## RESULTS

### Study participant characteristics

Twenty-nine women were enrolled in the study, one patient declined imaging after enrollment. Twenty-eight women with 29 tumors underwent  $^{18}\text{F}$ -ISO-1 PET/CT scans before initiation of any cancer directed therapy. Age range was 32-79 (median 55). Histology of the primary breast malignancy was invasive ductal carcinoma (IDC) in 21 (72%), invasive lobular carcinoma (ILC) in 4 (14%) and mixed IDC and ILC in 4 (14%). Study participant and tumor characteristics are summarized in Table 1. Most patients ( $n=18$ ) were early stage (1A and 2A). Mean tumor diameter (average of planar diameters) ranged from 7 to 81 mm.

### Measurements of $^{18}\text{F}$ -ISO-1 uptake and association with Ki-67

Tumor  $\text{SUV}_{\text{max}}$ ,  $\text{SUV}_{\text{max}}$ -to-normal-tissue ratios, DVR, mean tumor diameter, and histology of the primary breast malignancies for the entire cohort are provided in Supplemental Tables 1 and 2. Median

SUV<sub>max</sub> was 2.0 g/mL (range, 1.3–3.3 g/mL). Uptake in normal contralateral breast tissue ranged from 0.5 to 1.7 g/mL, with median 0.9 g/mL. SUV ratios of tumor-to-normal-breast had a unitless median value of 2.1 (range 1.04 to 4.63) while the tumor-to-normal-muscle median was 1.46 (range 0.60 to 3.58). Physiologic <sup>18</sup>F-ISO-1 uptake was seen in the liver, gallbladder, bowel and pancreas, and was similar to prior studies (1). <sup>18</sup>F-ISO-1-avid lesions were observed in the breast, axillary nodes, and extra-axillary nodes, as well as a previously unknown metastasis to the lung confirmed with <sup>18</sup>F-fluorodeoxyglucose PET/CT scan.

Representative images from tumors with low and high Ki-67 proliferative status (Ki-67 < or ≥20%) (29, 30) are shown in Figs. 1 and 2, respectively. Plots of tumor SUV<sub>max</sub> grouped by high and low Ki-67 (n=29) are depicted in Fig. 3A. Based on Wilcoxon rank-sum tests, there was a significant difference in SUV<sub>max</sub> between tumors stratified by low (n=15) and high (n=14) Ki-67, with SUV<sub>max</sub> in tumors with low Ki-67 significantly lower than for tumors with high Ki-67 (P=0.02) (Table 2). Since ductal cancers generally grow in a discrete spherical/round pattern, unlike the lobular subset that presents with more infiltrative linear strands of tumor cells loosely dispersed in the fibrous stroma of breast, we also assessed the association between <sup>18</sup>F-ISO-1 and cellular proliferation for the IDC subset (Fig. 3B). SUV<sub>max</sub> in IDC tumors with low Ki-67 (n=8) were significantly lower than that of SUV<sub>max</sub> in tumors with high Ki-67 (n=13; P=0.02) (Table 2).

The Wilcoxon rank-sum test analysis was repeated with a lower 14% Ki-67 threshold from an earlier 2011 St. Gallen meeting consensus (31) to stratify tumor proliferation as low (n=10) or high (n=19). The lower threshold analysis found <sup>18</sup>F-ISO-1 SUV<sub>max</sub>, SUV<sub>max</sub>/NBr, and DVR in tumors with low Ki-67 were significantly lower than in tumors with high Ki-67 (P≤0.02).

Spearman's rank analysis found <sup>18</sup>F-ISO-1 uptake via SUV<sub>max</sub> exhibited a significant positive association with Ki-67 proliferation scores across all breast cancers (ρ=0.46, P=0.01 in Fig. 4 and Table 3). Subsets of ER+ tumors and IDC tumors also showed significant correlations between SUV<sub>max</sub> and Ki-67 (ρ=0.51, P=0.02 and ρ=0.44, P=0.04, respectively).

Additional measurements of tumor-to-background, PVC SUV (to determine if correlations were dependent on lesion size), and tumor DVR were examined for associations with Ki-67. PVC SUV<sub>max</sub> was not associated with Ki-67 for all breast cancers ( $P>0.05$ ,  $n=29$ ), but was for invasive ductal cancers (Wilcoxon:  $P=0.001$ ; Spearman:  $\rho=0.53$ ,  $P=0.01$ ,  $n=21$ , in Tables 2 and 3). The  $^{18}\text{F}$ -ISO-1 SUV/NBr and SUV/NM were not significant for all cancers or for individual subtypes, but the correlation between SUV/NBr and Ki-67 had a trend towards significance ( $P=0.08$ ). Tumor DVR was not correlated with Ki-67 ( $P>0.1$ ).

## DISCUSSION

This prospective clinical trial of *in vivo*  $^{18}\text{F}$ -ISO-1 uptake in 28 breast cancer patients is the first focused trial of this tracer in breast cancer and demonstrates that SUV<sub>max</sub> correlates with *in vitro* Ki-67 index of proliferation while tumor-to-normal-breast ratio and DVR did not correlate with Ki-67 index, which supports the Dehdashti et al. results (1). The *in vivo* association in breast cancer is also consistent with prior *in vitro* cell culture studies as well as mouse studies utilizing a highly selective, optically labeled (fluorescent)  $\sigma\text{2R}$  ligand probe, SW120, wherein SW120 binding was positively correlated with Ki-67 (32).

While Ki-67 is a helpful biomarker, it requires tissue sampling and measurement can be confounded by intra-tumoral heterogeneity, poor reproducibility, and subjective readings (4). An imaging method for measuring tumor proliferation offers a non-invasive approach to assaying proliferation in breast and other cancers that takes into account the whole tumor and allows for repeated non-invasive measurements. This has been previously shown in breast cancer. For example, a multi-center trial tested the PET radiotracer 3'-deoxy-3'- $^{18}\text{F}$ -fluorothymidine ( $^{18}\text{F}$ -FLT) and measured uptake in primary breast cancer ( $n=51$  patients) in serial imaging over the course of neoadjuvant chemotherapy (33).  $^{18}\text{F}$ -FLT uptake correlated with post-therapy Ki-67 scores ( $P\leq 0.04$ ) on surgical specimens and serial uptake measures early in the course of treatment predicted response to therapy. However,  $^{18}\text{F}$ -FLT is trapped exclusively during S phase and not during G1, M, or G2, unlike Ki-67 and  $^{18}\text{F}$ -ISO-1, and may not fully represent tumor proliferative status (34). An imaging method more similar to Ki-67 labeling, such as  $^{18}\text{F}$ -ISO-1 PET, could assay all

components of tumor proliferative status, taking into account cells in all phases of the cell cycle. This might be especially helpful in evaluating response to cytostatic therapies, such as CDK 4/6 inhibitors. A recent preclinical study testing  $^{18}\text{F}$ -FLT and  $^{18}\text{F}$ -ISO-1 for monitoring breast cancer response to a combination of CDK 4/6 inhibition and endocrine-therapy concluded  $^{18}\text{F}$ -FLT was more sensitive to early changes in S-phase arising from combined treatment, while  $^{18}\text{F}$ -ISO-1 was better suited to quantitate delayed changes and to assess the impact of CDK4/6 inhibition on G1-phase to G0-phase arrest and overall tumor impact (35), supporting a potential clinical role for a tumor proliferative status tracer such as  $^{18}\text{F}$ -ISO-1.  $^{18}\text{F}$ -ISO-1 may also be useful as a companion diagnostic for sigma-2 targeted therapeutic applications, currently under study (34-36).

Our study of a single primary tumor type in a larger breast cancer cohort did not find a significant correlation between  $^{18}\text{F}$ -ISO-1 tumor-to-normal muscle ratios and Ki-67 ( $P=0.72$ ), unlike the Dehdasthi et al. report of a correlation between tumor-to-normal muscle ratio and Ki-67 index ( $P=0.003$ ) (1). This may be related to variability in normal muscle uptake, which may be more impactful for a less proliferative malignancy, such as breast cancer, with lower tumor uptake of radiotracer when compared to the more proliferative malignancies such as lymphoma and head and neck included in the Dehdashti study.

Our study has some limitations: breast cancer, as compared to many other solid tumor types, is a tumor with relatively low proliferation, and thus the range of SUV values is limited, especially for this largely ER+ tumor population, limiting our ability to assess correlation over the full spectrum of tumor proliferative status. PVC PET measures (PVC  $\text{SUV}_{\text{max}}$ ) only correlated with Ki-67 scores in patients with IDC ( $P<0.01$ ,  $n=21$ ). A potential explanation for this is that the PVC correction model (26) was based on all the tumors having an ideal spherical shape that is more applicable in IDC than ILC, where ILC tumors grow as ill-defined asymmetric lesions infiltrating the normal breast parenchyma in a linear single-file pattern. As such, partial-volume corrections for ILC might be expected to be less accurate than for IDC. Additionally, the gene coding for  $\sigma_2\text{R}$  was not known when the study was designed and conducted, so a pathologic assay for TMEM-97 was not prospectively planned in the IRB-approved study protocol. This limitation will be addressed in future studies. The uptake of  $^{18}\text{F}$ -ISO-1 in breast cancer is relatively low and

there is relatively high background activity seen on PET images in the fat tissue of the breast limiting its clinical value, particularly for low proliferating tumors. We also note that  $^{18}\text{F}$ -ISO-1 has more modest uptake and target-to-background compared to other tracers tested for application to breast cancer such as  $^{18}\text{F}$ -fluorodeoxyglucose and  $^{18}\text{F}$ -FLT, limiting its applicability. However, we note it is intended as a quantitative biomarker of proliferation, supported by our results, and not as a tool for detection and staging.  $^{18}\text{F}$ -ISO-1 instead may provide a basis for sigma-2 receptor based imaging of proliferation including potential for assessing response to cell-cycle targeted therapy. Further study of more potent sigma-2 receptor radiotracers in breast cancer patients is warranted with a goal of increasing the uptake of radiotracer in tumors relative to background tissue.

## **CONCLUSION**

Uptake of the sigma-2 ligand,  $^{18}\text{F}$ -ISO-1, correlates with an established tissue assay marker of tumor proliferative status, Ki-67. This supports the  $^{18}\text{F}$ -ISO-1 uptake findings of Dehdashti et. al., and can be used to design studies assessing  $^{18}\text{F}$ -ISO-1 or more potent sigma-2 targeting radiotracers *in vivo* for potential use in complementing other means of guiding cell-cycle targeted agents.

## **Financial support**

Dr. McDonald was supported by Susan G. Komen Foundation (CCR 16376362, SAC130060) and the American Roentgen Ray Society Scholar award. Dr. Doot was supported by the National Institute On Drug Abuse of the National Institutes of Health (K01DA040023). The work was supported by the National Center for Research Resources and the National Center for Advancing Translational Sciences, National Institutes of Health (UL1TR000003), U.S. Department of Energy (DE-SE0012476), Penn Radiology Department and NCI Cancer Center grant (P30 CA016520).

## **Disclosure**

Authors have no financial disclosures relevant to this work.

## **ACKNOWLEDGEMENTS**

We would like to thank those who have also contributed substantially to the work reported in the manuscript: Karen J. Palmer, Regan Sheffer, Federico Valdivieso, Noah Goodman, and Tiffany Dominguez.

### **Key points**

**QUESTION:** Can the novel radiotracer,  $^{18}\text{F}$ -ISO-1, provide a whole tumor measurement of breast cancer proliferative status?

**PERTINENT FINDINGS:** This exploratory study of  $^{18}\text{F}$ -ISO-1, demonstrates that this tracer provides a measure of tumor proliferative status (cycling cells) that correlates with a tissue based pathologic assay.

### **IMPLICATIONS FOR PATIENT CARE:**

- $^{18}\text{F}$ -ISO-1 PET/CT may be complementary to other methods for imaging cellular proliferation.
- $^{18}\text{F}$ -ISO-1 or more potent sigma-2 targeting radiotracers could be investigated further for possible use to help guide the use of cell-cycle targeted agents.

## REFERENCES

1. Dehdashti F, Laforest R, Gao F, et al. Assessment of cellular proliferation in tumors by PET using  $^{18}\text{F}$ -ISO-1. *J Nucl Med*. 2013;54:350-357.
2. Gerdes J, Lemke H, Baisch H, Wacker HH, Schwab U, Stein H. Cell cycle analysis of a cell proliferation-associated human nuclear antigen defined by the monoclonal antibody Ki-67. *J Immunol*. 1984;133:1710-1715.
3. Scholzen T, Gerdes J. The Ki-67 protein: from the known and the unknown. *J Cell Physiol*. 2000;182:311-322.
4. Dowsett M, Nielsen TO, A'Hern R, et al. Assessment of Ki67 in breast cancer: recommendations from the International Ki67 in Breast Cancer Working Group. *J Natl Cancer Inst*. 2011;103:1656-1664.
5. Goodson WH, 3rd, Moore DH, 2nd, Ljung BM, et al. The prognostic value of proliferation indices: a study with in vivo bromodeoxyuridine and Ki-67. *Breast Cancer Res Treat*. 2000;59:113-123.
6. Trihia H, Murray S, Price K, et al. Ki-67 expression in breast carcinoma: its association with grading systems, clinical parameters, and other prognostic factors--a surrogate marker? *Cancer*. 2003;97:1321-1331.
7. van Diest PJ, van der Wall E, Baak JP. Prognostic value of proliferation in invasive breast cancer: a review. *J Clin Pathol*. 2004;57:675-681.
8. Petit T, Wilt M, Velten M, et al. Comparative value of tumour grade, hormonal receptors, Ki-67, HER-2 and topoisomerase II alpha status as predictive markers in breast cancer patients treated with neoadjuvant anthracycline-based chemotherapy. *Eur J Cancer*. 2004;40:205-211.
9. Chang J, Ormerod M, Powles TJ, Allred DC, Ashley SE, Dowsett M. Apoptosis and proliferation as predictors of chemotherapy response in patients with breast carcinoma. *Cancer*. 2000;89:2145-2152.
10. Faneyte IF, Schrama JG, Peterse JL, Remijnse PL, Rodenhuis S, van de Vijver MJ. Breast cancer response to neoadjuvant chemotherapy: predictive markers and relation with outcome. *Br J Cancer*. 2003;88:406-412.
11. Ellis MJ, Suman VJ, Hoog J, et al. Ki67 proliferation index as a tool for chemotherapy decisions during and after neoadjuvant aromatase inhibitor treatment of breast cancer: results from the American College of Surgeons Oncology Group Z1031 Trial (Alliance). *J Clin Oncol*. 2017;35:1061-1069.
12. Goncalves R, DeSchryver K, Ma C, et al. Development of a Ki-67-based clinical trial assay for neoadjuvant endocrine therapy response monitoring in breast cancer. *Breast Cancer Res Treat*. Sep 2017;165:355-364.
13. Dowsett M, Smith IE, Ebbs SR, et al. Proliferation and apoptosis as markers of benefit in neoadjuvant endocrine therapy of breast cancer. *Clin Cancer Res*. 2006;12:1024s-1030s.

14. Mach RH, Smith CR, al-Nabulsi I, Whirrett BR, Childers SR, Wheeler KT. Sigma 2 receptors as potential biomarkers of proliferation in breast cancer. *Cancer research*. 1997;57:156-161.
15. Wheeler KT, Wang LM, Wallen CA, et al. Sigma-2 receptors as a biomarker of proliferation in solid tumours. *Br J Cancer*. Mar 2000;82:1223-1232.
16. Sai KK, Jones LA, Mach RH. Development of (18)F-labeled PET probes for imaging cell proliferation. *Curr Top Med Chem*. 2013;13:892-908.
17. Shoghi KI, Xu J, Su Y, et al. Quantitative receptor-based imaging of tumor proliferation with the sigma-2 ligand [<sup>18</sup>F]ISO-1. *PLoS One*. 2013;8:e74188.
18. Alon A, Schmidt HR, Wood MD, Sahn JJ, Martin SF, Kruse AC. Identification of the gene that codes for the sigma2 receptor. *Proc Natl Acad Sci U S A*. 2017;114:7160-7165.
19. Ding H, Gui XH, Lin XB, et al. Prognostic Value of MAC30 Expression in human pure squamous cell carcinomas of the lung. *Asian Pac J Cancer Prev*. 2016;17:2705-2710.
20. Han KY, Gu X, Wang HR, Liu D, Lv FZ, Li JN. Overexpression of MAC30 is associated with poor clinical outcome in human non-small-cell lung cancer. *Tumour Biol*. 2013;34:821-825.
21. Elmi A, Makvandi M, Weng CC, et al. Cell-proliferation imaging for monitoring response to CDK4/6 inhibition combined with endocrine-therapy in breast cancer: comparison of [<sup>18</sup>F]FLT and [<sup>18</sup>F]ISO-1 PET/CT. *Clin Cancer Res*. 2019;25:3063-3073.
22. Riad A, Zeng C, Weng CC, et al. Sigma-2 receptor/TMEM97 and PGRMC-1 increase the rate of internalization of LDL by LDL receptor through the formation of a ternary complex. *Sci Rep*. 2018;8:16845.
23. Tu Z, Xu J, Jones LA, et al. Radiosynthesis and biological evaluation of a promising sigma(2)-receptor ligand radiolabeled with fluorine-18 or iodine-125 as a PET/SPECT probe for imaging breast cancer. *Appl Radiat Isot*. 2010;68:2268-2273.
24. Kolthammer JA, Su KH, Grover A, Narayanan M, Jordan DW, Muzic RF. Performance evaluation of the Ingenuity TF PET/CT scanner with a focus on high count-rate conditions. *Phys Med Biol*. 2014;59:3843-3859.
25. Wahl RL, Jacene H, Kasamon Y, Lodge MA. From RECIST to PERCIST: evolving considerations for PET response criteria in solid tumors. *J Nucl Med*. 2009;50:122S-150S.
26. Peterson LM, Mankoff DA, Lawton T, et al. Quantitative imaging of estrogen receptor expression in breast cancer with PET and 18F-fluoroestradiol. *J Nucl Med*. 2008;49:367-374.
27. Logan J, Fowler JS, Volkow ND, Wang GJ, Ding YS, Alexoff DL. Distribution volume ratios without blood sampling from graphical analysis of PET data. *J Cereb Blood Flow Metab*. 1996;16:834-840.

28. Ichise M, Liow JS, Lu JQ, et al. Linearized reference tissue parametric imaging methods: application to [11C]DASB positron emission tomography studies of the serotonin transporter in human brain. *J Cereb Blood Flow Metab.* 2003;23:1096-1112.
29. Deluche E, Venat-Bouvet L, Leobon S, et al. Assessment of Ki67 and uPA/PAI-1 expression in intermediate-risk early stage breast cancers. *BMC Cancer.* 2017;17:662.
30. Coates AS, Winer EP, Goldhirsch A, et al. Tailoring therapies--improving the management of early breast cancer: St Gallen international expert consensus on the primary therapy of early breast cancer 2015. *Ann Oncol.* 2015;26:1533-1546.
31. Goldhirsch A, Wood WC, Coates AS, et al. Strategies for subtypes--dealing with the diversity of breast cancer: highlights of the St. Gallen international expert consensus on the primary therapy of early breast cancer 2011. *Ann Oncol.* 2011;22:1736-1747.
32. Zeng C, Vangveravong S, Jones LA, et al. Characterization and evaluation of two novel fluorescent sigma-2 receptor ligands as proliferation probes. *Molecular imaging.* 2011;10:420-433.
33. Kostakoglu L, Duan F, Idowu MO, et al. A phase II study of 3'-Deoxy-3'-18F-Fluorothymidine PET in the assessment of early response of breast cancer to neoadjuvant chemotherapy: results from ACRIN 6688. *J Nucl Med.* 2015;56:1681-1689.
34. Elmi A, McDonald ES, Mankoff D. Imaging tumor proliferation in breast cancer: current update on predictive imaging biomarkers. *PET Clin.* 2018;13:445-457.
35. McDonald ES, Mankoff DA, Mach RH. Novel strategies for breast cancer imaging: new imaging agents to guide treatment. *J Nucl Med.* 2016;57 (suppl 1):69s-74s.
36. McDonald ES, Mankoff J, Makvandi M, et al. Sigma-2 ligands and PARP inhibitors synergistically trigger cell death in breast cancer cells. *Biochem Biophys Res Commun.* 2017;486:788-795.

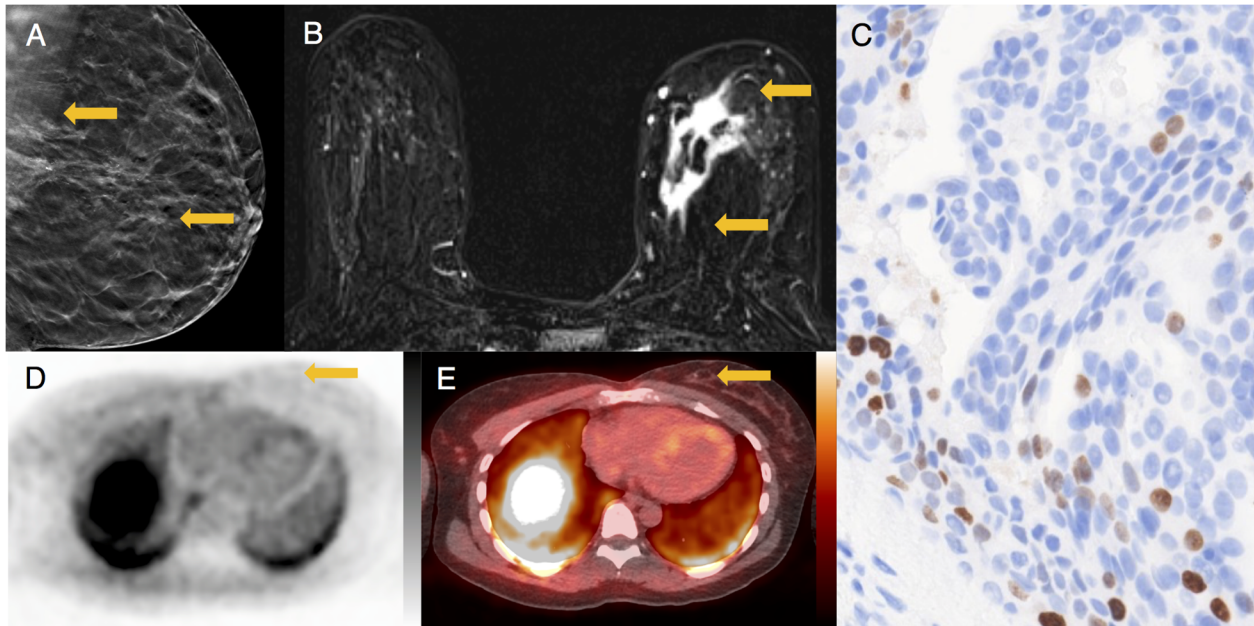


**FIGURE 1.** Tumor with low proliferative status. 42 year old woman with ER+/HER2- primary breast cancer. (A) Tomosynthesis mediolateral oblique projection demonstrates an irregular mass with spiculated margins and associated calcifications. (B) Axial contrast-enhanced T1 weighted subtraction image demonstrates an irregular mass in the medial breast with heterogeneous enhancement. (C) Ki-67 staining demonstrated a low percentage of actively dividing cells (11%) (Magnification 20x). (D) Axial  $^{18}\text{F}$ -ISO-1 demonstrating no qualitative uptake in the medial breast (arrow,  $\text{SUV}_{\text{max}}$  1.5 g/mL) (E) Corresponding fused  $^{18}\text{F}$ -ISO-1 PET/CT demonstrating a biopsy clip marking the site of malignancy (arrow). PET and PET/CT images scaled to 0-5 g/mL SUV, -160 to +240 HU.

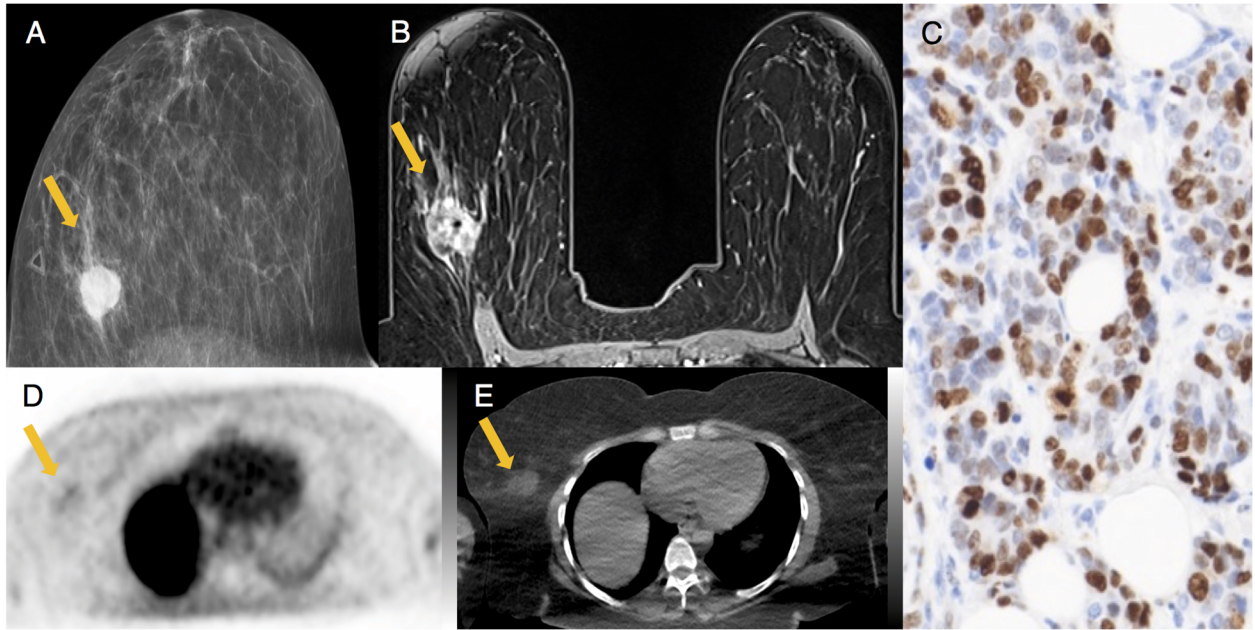


**FIGURE 2.** Tumor with high proliferative status. 40 year old woman with triple negative breast cancer. (A) Mammographic craniocaudal projection demonstrates a high density irregular mass with overlying palpable marker. (B) Axial contrast-enhanced T1 weighted image demonstrates that the mass is irregular with heterogeneous enhancement with central signal drop-out from biopsy marker. (C) Ki-67 staining demonstrated a high percentage of actively dividing cells (74%) (Magnification 20x). (D) Axial  $^{18}\text{F}$ -ISO-1 demonstrating qualitative uptake at the site of malignancy (arrow;  $\text{SUV}_{\text{max}}$  2.6 g/mL) (E) Corresponding CT image demonstrating an irregular mass (arrow). PET and CT images scaled to 0-5 g/mL SUV, -160 to +240 HU.

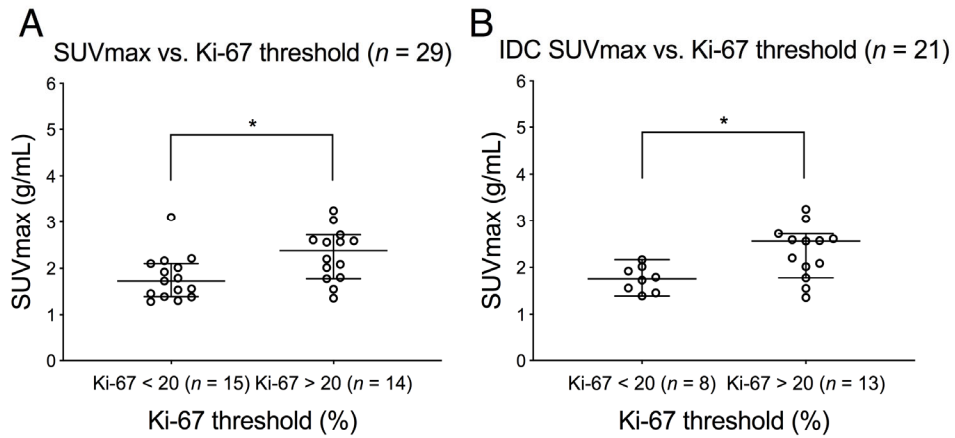


**FIGURE 3.** Plot of  $SUV_{max}$  in groups stratified by Ki-67 below or above 20. There was a significant difference in (A)  $SUV_{max}$  between patient tumors stratified by low ( $n = 15$ ) and high ( $n = 14$ ) Ki-67 values in all 29 tumors. (B)  $SUV_{max}$  stratified by low ( $n = 8$ ) and high ( $n = 13$ ) Ki-67 values restricted to invasive ductal carcinoma (IDC) ( $n = 21$ ) showed significant differences based on Ki-67 threshold. The center line of each distribution indicates the median value, error bars show 95% confidence interval of median. \* $P < 0.05$ .

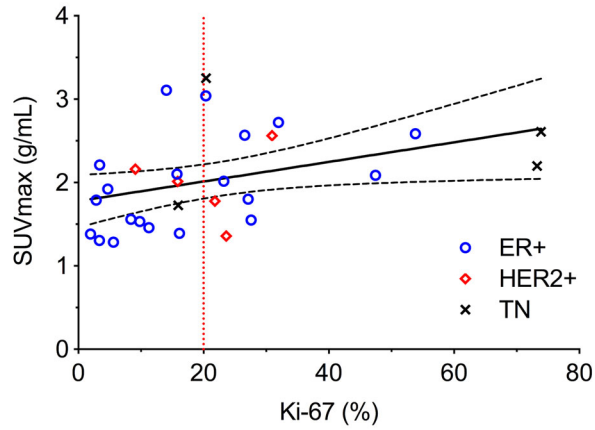


**FIGURE 4.** Scatter plots of  $SUV_{max}$  vs Ki-67 for ( $n = 29$ ) all tumor types (ER+ blue circles; HER2+ red diamonds; and triple negative (TN) black x's). Spearman tests found significant correlations with Ki-67 ( $\rho = 0.46$ ,  $P = 0.01$ ). Solid linear regression trend line and dashed 95% confidence intervals are included for reference.

**TABLE 1.** Study Participant and Tumor Characteristics

Characteristic	<i>n</i> (%)
Age	32-79 (median 55)
Sex	
Female	28 (28/28=100)
Race	
Caucasian	17 (17/28=61)
Black	9 (9/28=32)
Asian	1 (1/28=4)
Hispanic	1 (1/28=4)
Histology	
Invasive ductal carcinoma (IDC)	21 (21/29=72)
Invasive lobular carcinoma (ILC)	4 (4/29=14)
Mixed (IDC and ILC)	4 (4/29=14)
Histologic grade	
1	2 (2/29=7)
2	15 (15/29=52)
3	11 (11/29=38)
Not graded	1 (1/29=3)
AJCC tumor stage group*	
1A	9 (9/29=31)
2A	9 (9/29=31)
2B	7 (7/29=25)
3A	2 (2/29=7)
3B	1 (1/29=4)
IV	1 (1/29=4)
Receptor status	
ER <sup>†</sup> + or PR <sup>‡</sup> + / HER2 <sup>§</sup> -	20 (20/29=69)
HER2+ <sup>§</sup>	5 (5/29=17)
Triple negative (ER <sup>†</sup> -/PR <sup>‡</sup> -/HER2 <sup>§</sup> -)	4 (4/29=14)

\*Anatomic Stage Group from American Joint Committee on Cancer, Cancer Staging Manual, 8th Edition, DOI 10.1007/978-3-319-40618-3.

<sup>†</sup>Estrogen receptor.

<sup>‡</sup>Progesterone receptor.

<sup>§</sup>Human epidermal growth factor receptor 2.

**TABLE 2.** Wilcoxon's Rank-Sum Test of Tumor <sup>18</sup>F-ISO-1 Uptake Grouped by Ki-67 20% Threshold

Ki-67 versus	All Tumors ( <i>n</i> = 29), P	ER+* Tumors ( <i>n</i> = 20), P	IDC <sup>†</sup> Tumors ( <i>n</i> = 21), P
SUV <sub>max</sub>	0.02 <sup>‡</sup>	0.03 <sup>‡</sup>	0.02 <sup>‡</sup>
SUV <sub>max</sub> /NBr <sup>§</sup>	0.22	0.47	0.12
SUV <sub>max</sub> /NM <sup>  </sup>	0.95	0.79	1.00
DVR <sup>¶</sup>	0.27	0.43	0.12
PVC <sup>#</sup> SUV <sub>max</sub>	0.16	0.57	< 0.01 <sup>‡</sup>

\*Estrogen receptor positive.

<sup>†</sup>Invasive ductal carcinoma.

<sup>‡</sup>P < 0.05.

<sup>§</sup>Normal contralateral breast (NBr).

<sup>||</sup>Normal left latissimus dorsi muscle (NM).

<sup>¶</sup>Distribution volume ratio (DVR).

<sup>#</sup>Partial volume corrected (PVC).

**TABLE 3.** Spearman Rank Correlations between <sup>18</sup>F-ISO-1 Uptake and Ki-67

Ki-67 versus	All Tumors (n = 29)		Estrogen Receptor+ (n = 20)		Invasive Ductal Carcinoma (n = 21)	
	ρ	P	ρ	P	ρ	P
SUV <sub>max</sub>	0.46	0.01*	0.51	0.02*	0.44	0.04*
SUV <sub>max</sub> /NBr <sup>†</sup>	0.33	0.08	0.32	0.17	0.27	0.24
SUV <sub>max</sub> /NM <sup>‡</sup>	0.07	0.72	0.06	0.79	-0.09	0.68
DVR <sup>§</sup>	0.30	0.12	0.33	0.15	0.25	0.28
PVC <sup>  </sup> SUV <sub>max</sub>	0.22	0.25	0.17	0.47	0.53	0.01*

\*P &lt; 0.05.

<sup>†</sup>Normal contralateral breast (NBr).<sup>‡</sup>Normal left latissimus dorsi muscle (NM).<sup>§</sup>Distribution volume ratio (DVR).<sup>||</sup>Partial volume corrected (PVC).

## SUPPLEMENTAL TABLES 1 and 2

### Breast Cancer <sup>18</sup>F-ISO-1 Uptake as a Marker of Proliferation Status.

Elizabeth S. McDonald, MD, PhD<sup>1\*</sup>, Robert K. Doot, PhD<sup>1\*</sup>, Anthony J. Young, BS<sup>1</sup>, Erin K. Schubert, BS<sup>1</sup>, Julia Tchou, MD, PhD<sup>2</sup>, Daniel A. Pryma, MD<sup>1</sup>, Michael D. Farwell, MD<sup>1</sup>, Anupma Nayak, MBBS, MD<sup>3</sup>, Amy Ziober<sup>3</sup>, Michael D. Feldman, MD, PhD<sup>3</sup>, Angela DeMichele, MD<sup>4</sup>, Amy S. Clark, MD<sup>4</sup>, Payal D. Shah, MD<sup>4</sup>, Hsiaoju Lee, PhD<sup>1</sup>, Sean D. Carlin, PhD<sup>1</sup>, Robert H. Mach, PhD<sup>1</sup>, David A. Mankoff, MD, PhD<sup>1</sup>

**Author affiliations:** <sup>1</sup>Department of Radiology, <sup>2</sup>Department of Surgery, <sup>3</sup>Department of Pathology and Laboratory Medicine, <sup>4</sup>Department of Medicine, Perelman School of Medicine, University of Pennsylvania  
\*Contributed equally to this work as co-first authors.

**SUPPLEMENTAL TABLE 1. Tumor SUV and SUV-to-Background Ratios**

Patient ID	SUV <sub>max</sub> (g/mL)	SUV <sub>max</sub> /NBr* Unitless	SUV <sub>max</sub> /NM <sup>†</sup> Unitless	DVR <sup>‡</sup> Unitless	PVC <sup>§</sup> SUV <sub>max</sub> (g/mL)
1	2.61	2.12	1.40	1.87	2.77
2	2.02	2.21	1.57	2.08	2.22
3	1.78	1.65	1.11	1.43	1.97
4	2.21	1.59	1.16	1.42	3.43
5	1.55	1.93	0.88	1.79	1.81
6	1.56	1.86	1.45	1.77	1.92
7	2.09	2.84	2.19	2.35	2.27
8	1.31	1.04	0.60	0.91	1.42
10	2.10	3.98	3.56	3.68	2.45
11	1.80	1.14	0.85	0.77	1.83
12	2.01	2.47	2.18	2.11	2.16
13	2.57	1.54	0.98	1.46	2.78
14	3.11	4.38	3.58	4.46	4.87
14b	1.53	2.16	1.76	2.01	2.90
15	1.46	1.77	0.95	1.63	1.53
16	2.56	2.66	1.46	2.49	2.74
17	1.92	2.24	2.24	2.06	2.16
18	1.39	1.46	1.18	1.22	1.44
19	2.72	3.47	1.95	2.81	3.04
20	1.73	2.20	1.80	1.89	1.83
21	2.59	1.85	0.82	1.64	2.72
22	2.16	1.68	0.97	1.54	2.26
23	2.20	2.27	1.67	2.00	2.34
24	1.38	1.66	1.12	1.50	1.69
25	1.79	1.65	1.48	1.61	1.91
26	1.36	2.18	1.57	1.88	2.71
27	1.29	1.29	0.73	1.06	3.34
28	3.04	2.97	1.85	2.58	3.27
29	<u>3.25</u>	<u>4.63</u>	<u>3.08</u>	<u>3.83</u>	<u>3.54</u>
Mean:	2.04	2.24	1.59	1.99	2.46
Median:	2.01	2.12	1.46	1.87	2.27
Standard deviation:	0.57	0.91	0.78	0.84	0.76

\*Normal contralateral breast (NBr).

<sup>†</sup>Normal left latissimus dorsi muscle (NM).<sup>‡</sup>Distribution volume ratio (DVR).<sup>§</sup>Partial volume corrected (PVC).

**SUPPLEMENTAL TABLE 2: Patient Ki-67 and Tumor Histology**

Patient ID	K-67 (%)	MTD [mm]	Type	Receptor	Grade
1	73.90	33.67	IDC <sup>†</sup>	TN <sup>‡</sup>	3
2	23.23	19.67	IDC <sup>†</sup>	ER+ <sup>§</sup>	2
3	21.80	17.67	IDC <sup>†</sup>	HER2+ <sup>  </sup>	3
4	3.40	11.67	ILC <sup>¶</sup>	ER+ <sup>§</sup>	N/A
5	27.58	16.67	IDC <sup>†</sup>	ER+ <sup>§</sup>	3
6	8.38	15.33	IDC <sup>†</sup>	ER+ <sup>§</sup>	2
7	47.45	22.00	IDC <sup>†</sup>	ER+ <sup>§</sup>	3
8	3.37	10.00	ILC <sup>¶</sup>	ER+ <sup>§</sup>	1
10	15.75	18.67	M <sup>#</sup>	ER+ <sup>§</sup>	2
11	27.11	25.67	M <sup>#</sup>	ER+ <sup>§</sup>	2
12	15.88	23.33	IDC <sup>†</sup>	HER2+ <sup>  </sup>	3
13	26.56	18.33	IDC <sup>†</sup>	ER+ <sup>§</sup>	3
14	14.06	14.00	M <sup>#</sup>	ER+ <sup>§</sup>	2
14b	9.82	11.33	ILC <sup>¶</sup>	ER+ <sup>§</sup>	2
15	11.25	47.33	IDC <sup>†</sup>	ER+ <sup>§</sup>	2
16	30.94	27.33	IDC <sup>†</sup>	HER2+ <sup>  </sup>	2
17	4.69	18.67	IDC <sup>†</sup>	ER+ <sup>§</sup>	3
18	16.15	24.33	IDC <sup>†</sup>	ER+ <sup>§</sup>	3
19	31.96	20.33	IDC <sup>†</sup>	ER+ <sup>§</sup>	2
20	15.95	29.00	IDC <sup>†</sup>	TN <sup>‡</sup>	2
21	53.84	27.33	IDC <sup>†</sup>	ER+ <sup>§</sup>	3
22	9.11	54.33	IDC <sup>†</sup>	HER2+ <sup>  </sup>	2
23	73.26	26.00	IDC <sup>†</sup>	TN <sup>‡</sup>	2
24	1.94	15.00	M <sup>#</sup>	ER+ <sup>§</sup>	2
25	2.84	20.00	IDC <sup>†</sup>	ER+ <sup>§</sup>	1
26	23.63	11.00	IDC <sup>†</sup>	HER2+ <sup>  </sup>	2
27	5.62	7.33	ILC <sup>¶</sup>	ER+ <sup>§</sup>	2
28	20.36	36.33	IDC <sup>†</sup>	ER+ <sup>§</sup>	3
29	<u>20.40</u>	<u>81.00</u>	IDC <sup>†</sup>	TN <sup>‡</sup>	3
Mean:	22.08	24.25			
Median:	16.15	20.00			
Standard deviation:	19.00	15.19			

\*Mean tumor diameter (MTD).

†Invasive Ductal Carcinoma (IDC).

‡Triple negative breast cancer (TN).

§Estrogen receptor positive (ER+).

|| Human epidermal growth factor receptor 2 (HER2+).

¶Invasive lobular carcinoma (ILC).

#Mixture of IDC and ILC (M).